Electronic Supplementary Information for

Bacterial nanocellulose and CdTe quantum dots: assembled nanopaper for heavy metal detection in aqueous solution

Inés Hernández Celi, Paula T. Peña González,[a] and Carlos A. Martínez Bonilla,*[a]

[a]Grupo de Investigación en Nuevos Materiales y Energías Alternativas – GINMEA, Semillero en Nuevos Materiales – SENUMA, Universidad Santo Tomas, Bucaramanga Colombia.

Present address: Universidad Santo Tomas, seccional Bucaramanga, Facultad de Química Ambiental, Santander, Colombia.

Corresponding author e-mail: camartinez885@gmail.com, carlos.andres.martinez.bonilla@umontreal.ca

Table of Contents **Pages**

1. Calculations of QDs concentration used in the chemosensor assembly. S2

2. Calculations for determining QDs concentration and retention in the BNC. S3

3. Chemosensor assembly: DTZ/QDs/BNC S4

4. MATLAB programming: RGB analysis. S10

5. Comparative analysis: chemosensor vs Atomic Absorption AAS S12

6. Normalized fluorescence of the chemosensor in the presence of possible interferences S14

1. Calculations of QDs concentration used in the chemosensor assembly.

The absorption properties of CdTe-TGA QDs are related to their size and diameter, as described by the equation proposed by Yu et al.[1]

Equation 1. Error! Reference source not found.

where λ is the maximum absorption. The extinction coefficient can be determined experimentally using the following equation:

Equation 2. Error! Reference source not found.

where D is the QD diameter. Finally, by applying Beer's law (Equation 3), it is possible to determine the concentration of the CdTe QDs:

Equation 3. Error! Reference source not found.

In Equation 3, A corresponds to the absorbance at the position of the first absorption peak of the excitons in a given sample, ∈ is the extinction coefficient (M^{-1} cm^{-1}), C is the molar concentration of the QDs, and L is the path length of the radiation beam used to record the absorption spectrum, which was 1,0 cm in the present investigation. Concentrations ranging from approximately 33 μM to 0.8 μM were evaluated, with the concentrations chosen to preserve the fluorescence of the QDs.

Entry	Excitonic peak (nm)	Absorbance (u.a)	Diameter (nm)	Extinction Coefficient ($M^{-1}cm^{-1}$)	Concentration CdTe (μM)
Solution 1	519.79	2.8607	2.7937	88666.1	32.3
Solution 2	510.69	0.7379	2.6035	76355.5	9.7
Solution 3	510.09	0.1864	2.5898	75504.8	2.5
Solution 4	505.79	0.0533	2.4869	69285.3	0.8

2. Calculations for determining QDs concentration and retention in the BNC.

The UV-Vis spectra of the solutions remaining after assembly were obtained for concentration calculations. The previously described equations were used for these calculations.

Figure S1. *UV-Vis spectra of the CdTe solutions after the preparation of the chemosensor.*

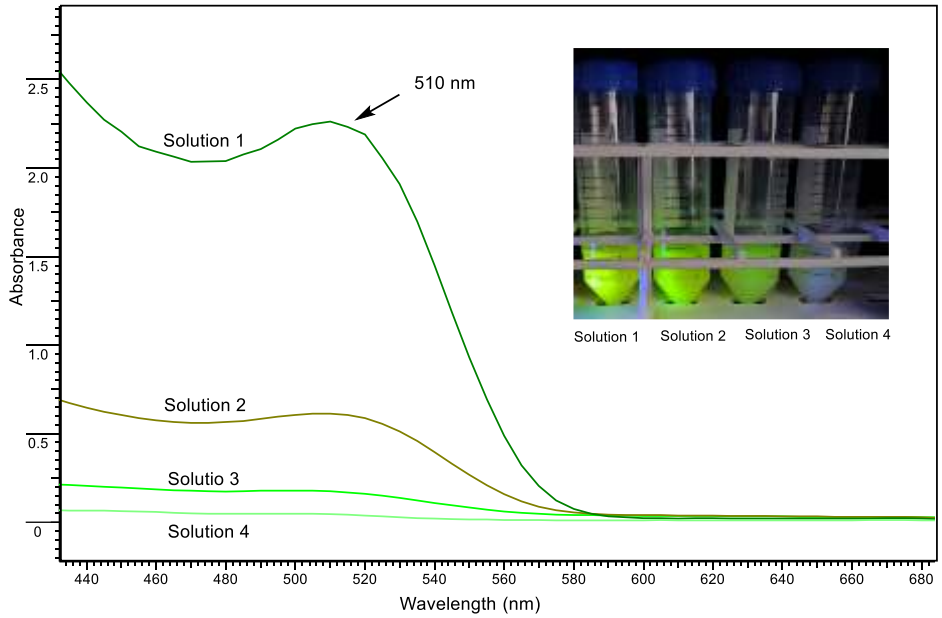

Table S1. *CdTe solution concentrations.*

Entry	Excitonic peak (nm)	Absorbance (u.a)	Diameter (nm)	Extinction Coefficient ($M^{-1}cm^{-1}$)	Concentration CdTe (µM)
Solution 1	509.92	2.2604	2.5858	75263.0	30
Solution 2	509.73	0.6139	2.5815	74992.3	8.2
Solution 3	510	0.1765	2.5877	75376.8	2.3
Solution 4	505	0.0471	2.4671	68121.0	0.7

The obtained results demonstrate a clear reduction in the concentration of the CdTe QDs solutions employed for the chemosensor assembly, suggesting that the nanomaterial's adsorption on the surface of the NCB support occurred. It is worth noting that lower adsorption of the nanomaterial on the support matrix occurs at low QD concentrations. Moreover, it should be emphasized that concentrations higher than 33 µM did not generate significant changes in the fluorescence of the chemosensor.

3. Chemosensor assembly: DTZ/QDs/BNC.

DTZ/QDs/BNC chemosensor assembly was performed because of the individual response of both sensitizing agents and their joint response when subjected to HMs solutions. The results obtained for the identification of the detection limit of QDs against mercury (Hg^{2+}) as the analyte of interest are detailed below. Each test was performed in triplicate in a 96-well microplate.

Figure S2. *Evaluation of QDs solutions against Hg^{2+} with a concentration between 1 mM to 1 nM.*

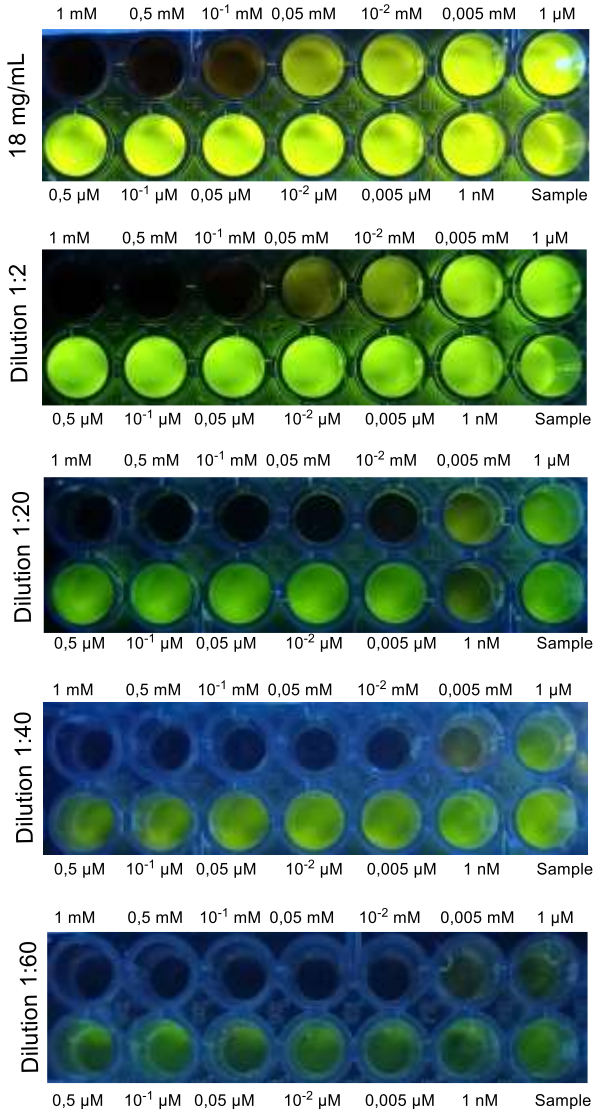

The above results indicate that for the 1:60 dilution, there is an appropriate range of response, highlighted by a progressive reduction in fluorescence in the range of concentrations of the HMs evaluated, recognizing significant changes between the responses obtained at 1 mM, 1 µM, and 1 nM concentrations.

The responses of the QDs/BNC chemosensor to various heavy metals are highlighted below.

Table S2. *QDs/BNC chemosensor response to MPs.*

HMs	Concentration		
	1 mM	1 µM	1 nM
As^{3+}	-	-	-
Cr^{6+}	+	+	+
Ag^{+}	+	+	+
Cu^{2+}	+	+	-
Hg^{2+}	+	+	+
Ni^{2+}	+	-	-
Pb^{2+}	+	+	+
Zn^{2+}	+	-	-

Retrieved from Generación de quimiosensores del nanocomposito celulosa bacteriana/puntos cuánticos como indicador de contaminación por metales pesados en muestras acuosas [2]

Similar tests were performed with a 1 mM dithizone (DTZ) solution, which was subjected to the presence of the heavy metals evaluated using the QDs/BNC chemosensor.

Table S3. *Response of the 1 mM DTZ solution vs. HMs.*

DTZ Concentration	HMs Analyzed [1 mM]	Photographic Record	Remarks	Response
1 mM	As^{3+}		Dark green	Negative
	Cr^{6+}		Purple, a precipitate is generated	Positive
	Ag^{+}		Black	Positive
	Cu^{2+}		Dark red	Positive

DTZ Concentration	HMs Analyzed [1 mM]	Photographic Record	Remarks	Response
	Hg^{2+}		Gray	Positive
	Ni^{2+}		Orange	Positive
	Pb^{2+}		Red, a precipitate is generated	Positive
	Zn^{2+}		Pink	Positive

Knowing the individual responses of each sensitizing agent, a qualitative analysis of the DTZ/QD solution was performed considering the solubility of the dithizone, the ease of subsequent assembly of the chemosensor to the support matrix (CNB), and the conservation of the properties under visible light of the DTZ and UV light of the QDs. During this analysis, it was necessary to corroborate that the behavior of the QDs against the MPs being analyzed was the same as when they were in the QDs/NCB nanocomposite, ruling out any effect of the luminescent properties of DTZ. Considering the above, a 4:1 solution of DTZ/QDs was prepared, with the former solubilized in isopropanol (1 mM concentration) and the latter solubilized in water. During the preparation of the solution, DTZ rapidly changed its coloration from dark green to yellow when it came into contact with water; however, there was no effect on the fluorescence of the QDs. On the other hand, the behavior of the solution prepared under UV light showed a similar response to that of the previously prepared chemosensor against metals of interest such as mercury, silver, copper, and chromium (Figure S3).

Figure S3. *Qualitative analysis of DTZ/QDs solution vs. MPs (a) under UV light, and (b) under natural light.*

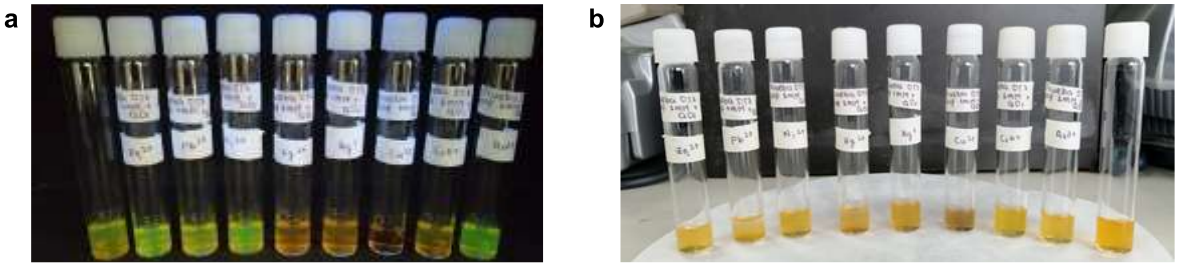

Notes: (a) From left to right are the standard solution (DTZ/QDs) and HM solutions of zinc, lead, nickel, mercury, silver, copper, chromium, and arsenic. **(b)** From left to right are the PM solutions of zinc, lead, nickel, mercury, silver, copper, chromium, arsenic, and the standard solution (DTZ/QDs).

Table S3. *DTZ/QDs solution response to HMs.*

HMs (1 mM)	Photographic Record	Observations	UV light response	Natural light response
As^{3+}	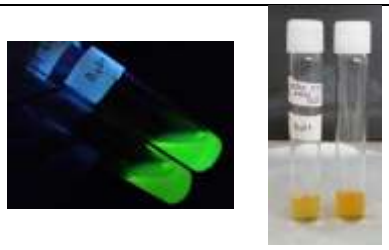	Final staining yellow/orange	Negative	Negative
Cr^{6+}	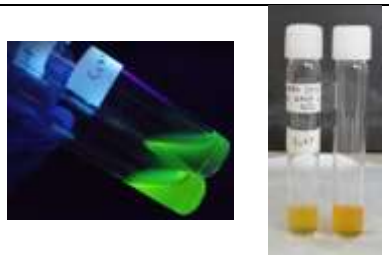	Final staining reduction in fluorescence of QDs	Positive	Positive
Cu^{2+}		Final staining brown, quenching of the fluorescence of the QDs	Positive	Positive
Ag^{+}	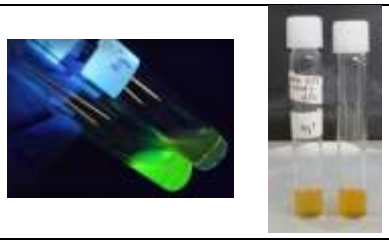	Final staining orange a shade darker, reduction in fluorescence of QDs	Positive	Positive

HMs (1 mM)	Photographic Record	Observations	UV light response	Natural light response
Ni^{2+}	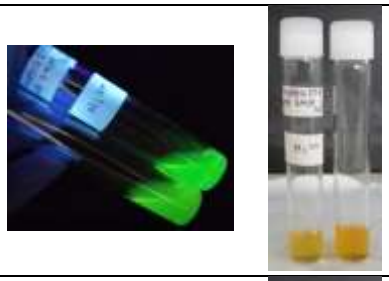	Final staining yellow/orange	Negative	Negative
Hg^{2+}	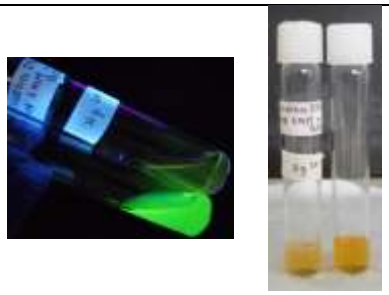	Final staining orange/red, reduction in color intensity, generation of precipitate, quenching of fluorescence of QDs	Positive	Positive
Pb^{2+}		Final staining yellow/orange, a precipitate is generated	Positive	Positive
Zn^{2+}	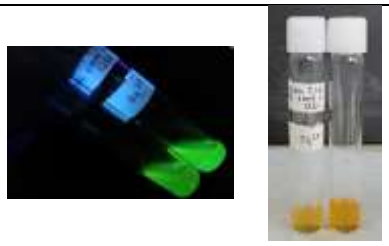	Final staining yellow/orange	Negative	Negative

It is necessary to emphasize that the tests under natural light had difficulty that the coloration of the solution varied in the scale of yellow and orange. Despite this, the selectivity of the QDs/DTZ solution against metals such as copper, where a total quenching of the fluorescence and significant variations in its color under natural light are also highlighted.

Finally, the assembly of the DTZ/QDs/BNC chemosensor was performed by two different routes or assays, described as follows:

Assay 1. Approximately 1 g of BNC was taken on wet weight which was mixed with 2.5 mL of CdTe-TGA QDs and 1 mL of DTZ. The mixture was sonicated for 5 min and filtered under a vacuum to obtain the chemosensor films. These films were dried at room temperature.

Assay 2. Approximately 1 g of BNC was taken by wet weight and mixed with 2.5 mL of CdTe-TGA QDs. The mixture was sonicated for 5 min and filtered under vacuum to obtain the QDs/BNC films. Finally, the films were impregnated with 1 mM DTZ solution and dried at room temperature.

Figure S4. *DTZ/QDs/BNC assembled chemosensors.*

The final physical appearance of optimal QDs/BNC chemosensor:

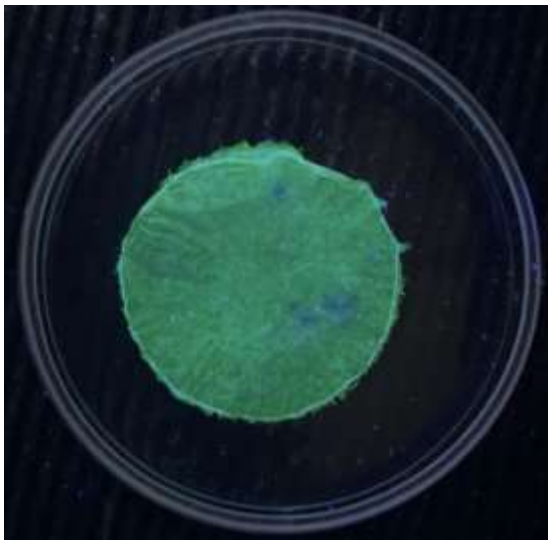

Entire nanopaper (~ 5 cm diameter)

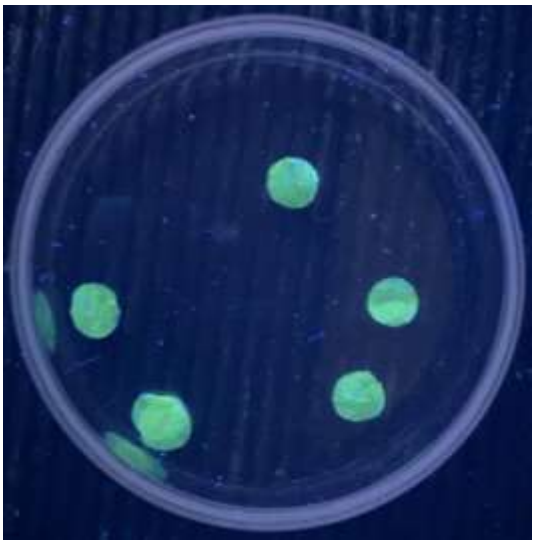

Nanopaper circles were cut and used in the 96-well microplate heavy metal assay.

4. MATLAB programming: RGB analysis.

The color analysis was performed using a Matlab tool where, through the established line of code, the image was read, from which the channel or fraction corresponding to the presence of green was extracted, and from there the image was transformed into the binary system, in black and white scale according to the presence of the color of interest. For the development of the analysis, it was necessary to have the same layout for each of the chemosensor fractions used in the analysis of HMs, and at the same time, to have photos of each of the tests before and after detection with equal pixel size. Each of the above parameters, allowed to automate the process of detection and estimation of the presence of green color in each of the wells or tests performed, where the program, according to the size and distances evidenced between well and well, automatically performed the cutting of each of the sections corresponding to the tests performed in order to carry out the processing and obtain each of the numerical results related to the quantification of the presence of the fraction of green before and after the evaluation.

In consideration, the following is the line of code established for image processing by RGB analysis.

Figure S5. *Matlab programming code for image processing.*

```
clc
clear all
close all

%Preprosesamiento
file_A = 'C:\Users\Paula Tatiana Peña G\OneDrive\ImAgenes\1.jpg';
file_D = 'C:\Users\Paula Tatiana Peña G\OneDrive\Imagenes\Ensayos 1,3 mg en 10 mL\Prueba 2\Despues\IMG_20220131_15
%Leer la imagen
f = imread(file_A);
figure;
imshow(f);
%Canal verde
Im_G = f(:,:,2);
figure;
imshow(Im_G);
%Imagen en binario
BW = imbinarize(Im_G);
im_filt = medfilt2(BW);
figure;
imshow(im_filt);

figure;
%Regiones de interes
ROI_1 = imcrop(im_filt ,[77.5 70.5 54 68]);
ROI_2 = imcrop(im_filt,[283.5 67.5 54 68]);
ROI_3 = imcrop(im_filt,[505.5 66.5 54 68]);
ROI_4 = imcrop(im_filt,[76.5 284.5 54 68]);
ROI_5 = imcrop(im_filt,[296.5 284.5 54 68]);
ROI_6 = imcrop(im_filt,[520.5 284. 54 68]);
ROI_7 = imcrop(im_filt,[82.5 489.5 54 68]);
ROI_8 = imcrop(im_filt,[299.5 489.5 54 68]);
ROI_9 = imcrop(im_filt,[520.5 498.5 54 68]);

% figure
subplot(3,3,1);
imshow(ROI_1);
subplot(3,3,2);
imshow(ROI_2);
subplot(3,3,3);
imshow(ROI_3);
subplot(3,3,4);
imshow(ROI_4);
subplot(3,3,5);
imshow(ROI_5);
subplot(3,3,6);
imshow(ROI_6);
```

```
47
48 -    subplot(3,3,7);
49 -    imshow(ROI_7);
50 -    subplot(3,3,8);
51 -    imshow(ROI_8);
52 -    subplot(3,3,9);
53 -    imshow(ROI_9);
54
55
56     % procesamiento
57 -    valores = [bwarea(ROI_1) bwarea(ROI_2) bwarea(ROI_3) bwarea(ROI_4) bwarea(ROI_5) bwarea(ROI_6) bwarea(ROI_7) bwarea
```

5. Comparative analysis: chemosensor vs Atomic Absorption AAS

An aging experiment was performed to detect the release of Cd from the core of the QDs from the chemosensor. The assembled nanopaper was immersed in distilled water and monitored for a period of 3 months using AAS. After monitoring, no Cd was observed in the remaining solution with a Cd LOD of 0,03 mg/L

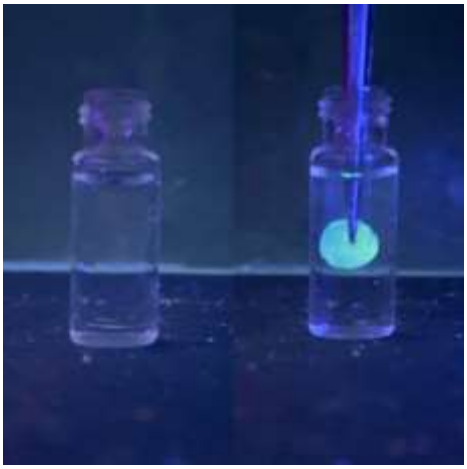

DI water under λ =254 nm

Nanopaper + DI water under λ =254 nm, t = 0 s

Nanopaper + DI water under λ =254 nm after 1 month.

For the comparison between both techniques, the HMs with favorable results for detection using the designed chemosensor were initially selected. In this order of ideas, we worked with metals such as Cu^{2+}, Pb^{2+}, and Hg^{2+}, since they also generated a positive response to the DTZ solution, being favorable candidates for detection under natural light and UV light. Considering the above, we proceeded to identify the quantification limit of the atomic absorption equipment (Thermo Scientific 3000) for each of the selected HMs, obtaining the following graphs.

Figure S6. *AAS fitting curve for copper (Cu^{2+}).*

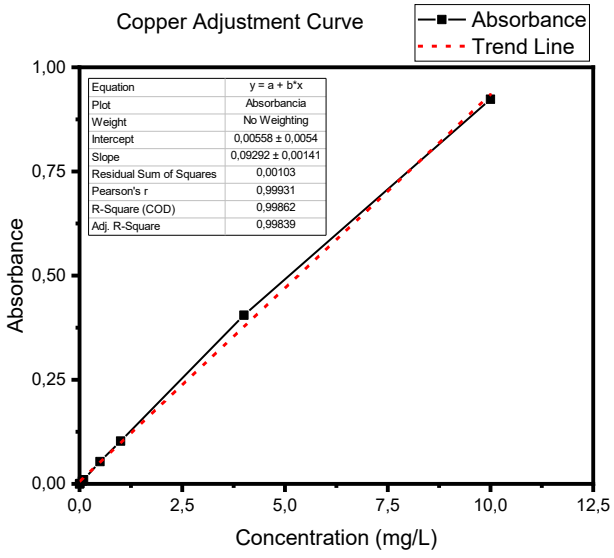

Figure S7. *AAS fitting curve for lead (Pb^{2+}).*

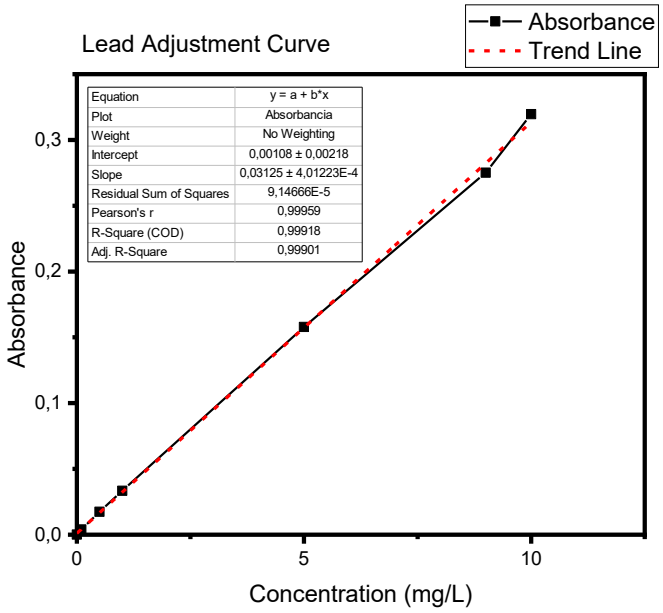

Figure S8. *AAS fitting curve for mercury (Hg^{2+}).*

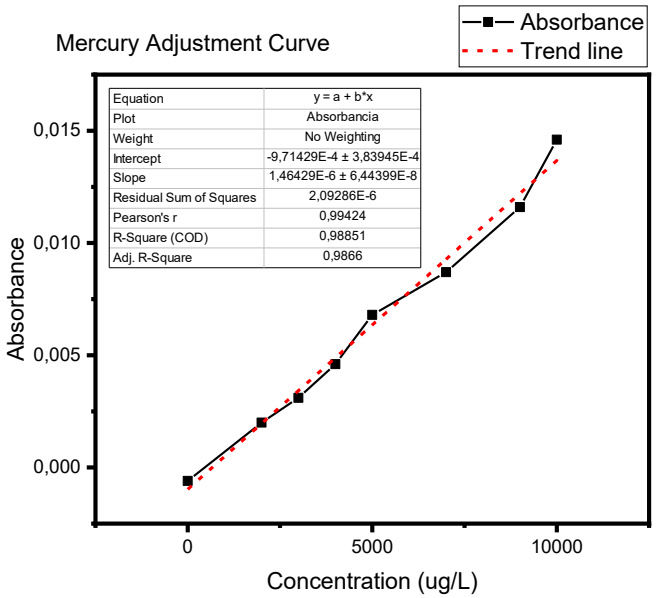

For each of the graphs corresponding to the HMs analyzed, the limits of quantification of the analysis equipment were determined, obtaining the results shown below.

Table S4. *Limits of detection by AAS for each of the analyzed HMs*

Analyzed HMs	**Concentration Limit of detection by AAS**	
	Parts per million (mg/L)	**Nanomolar (nM)**
Cu^{2+}	0,01	1101

Pb^{2+}	0,05	241
Hg^{2+}	1	4985

Each of the results obtained by atomic absorption was compared with the detection limits established for the CdTe QDs chemosensor, results that were processed by a color or RGB analysis, corresponding to the evaluation of the color space that is established in the three primary colors, being red, green, and blue.

6. Normalized fluorescence of the chemosensor in the presence of possible interferences.

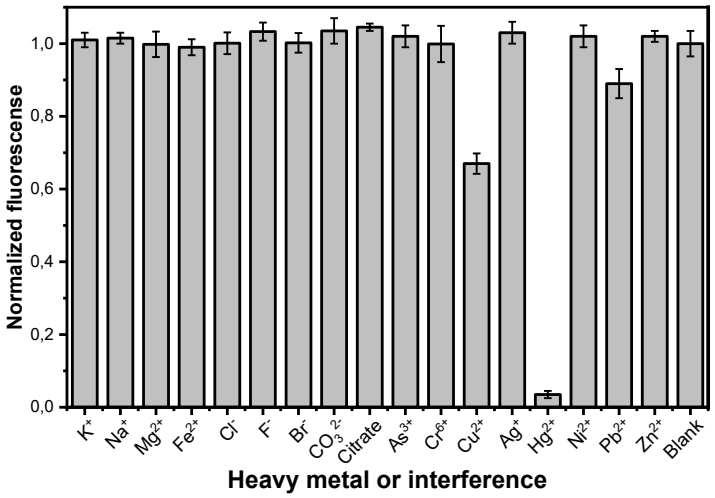

References

(1) Yu, W. W.; Qu, L.; Guo, W.; Peng, X. Experimental Determination of the Extinction Coefficient of CdTe, CdSe, and CdS Nanocrystals. *Chem. Mater.* **2003**, *15* (14), 2854–2860. https://doi.org/10.1021/cm034081k.

(2) Peña, P. Generación de Quimiosensores Del Nanocomposito Celulosa Bacteriana/Puntos Cuánticos Como Indicador de Contaminación Por Metales Pesados En Muestras Acuosas, Universidad Santo Tomás, 2020. https://repository.usta.edu.co/handle/11634/32504.